

Gas Absorption Detected from the Edge-on Debris Disk Surrounding HD32297

Seth Redfield¹

*Department of Astronomy and McDonald Observatory, University of Texas, Austin, TX,
78712*

sredfield@astro.as.utexas.edu

ABSTRACT

Near-infrared and optical imaging of HD32297 indicate that it has an edge-on debris disk, similar to β Pic. I present high resolution optical spectra of the Na I doublet toward HD32297 and stars in close angular proximity. A circumstellar absorption component is clearly observed toward HD32297 at the stellar radial velocity, which is not observed toward any of its neighbors, including the nearest only 0'9 away. An interstellar component is detected in all stars >90 pc, including HD32297, likely due to the interstellar material at the boundary of the Local Bubble. Radial velocity measurements of the nearest neighbors, BD+07 777s and BD+07 778, indicate that they are unlikely to be physically associated with HD32297. The measured circumstellar column density around HD32297, $\log N_{\text{NaI}} \sim 11.4$, is the strongest Na I absorption measured toward any nearby main sequence debris disk, even the prototypical edge-on debris disk, β Pic. Assuming that the morphology and abundances of the gas component around HD32297 are similar to β Pic, I estimate an upper limit to the gas mass in the circumstellar disk surrounding HD32297 of $\sim 0.3 M_{\oplus}$.

Subject headings: circumstellar matter — ISM: structure — line: profiles — planetary systems: protoplanetary disks — stars: early-type — stars: individual (HD32297)

1. Introduction

Debris disk systems provide a look at an intermediate stage of stellar system evolution. They represent the transition between the early formation of stars and planets in a primordial

²Hubble Fellow.

protoplanetary disk as seen toward pre-main sequence stars, and the mature stage of an evolved system, like our solar system, which is clear of all primordial material and retains only a hint of secondary products (e.g., zodiacal dust), the final remnants of the stellar and planetary formation process. Although a debris disk has lost most of its primordial material, the observed infrared luminosity of circumstellar dust, caused by collisions of planetismals and other small bodies, is typically several orders of magnitude larger than estimated for the Kuiper and asteroid belts in our solar system (Backman & Paresce 1993). Ever since the detection of dusty circumstellar material around main sequence stars via infrared excesses (Aumann et al. 1984), researchers have been looking for circumstellar gas phase absorption (Hobbs et al. 1985). Of the initial major infrared excess main sequence stars, only β Pic showed gas phase absorption in optical absorption lines (e.g., Ca II and Na I), due to its disk morphology and edge-on orientation (Smith & Terrile 1984). Such an orientation provides a unique opportunity to simultaneously measure both the dust and gas components of a debris disk, at an interesting transition near the end of stellar and planetary formation.

Only a few other edge-on debris disks have been found since, including β Car (Lagrange-Henri et al. 1990b), HD85905 (Welsh et al. 1998), HR10 (Lagrange-Henri et al. 1990a), and AU Mic (Kalas, Liu, & Matthews 2004; Roberge et al. 2005). Redfield, Kessler-Silacci, & Cieza (2007) observed β Car, HD85905, HR10 with the *Spitzer Space Telescope* and did not find strong infrared excesses toward any of them, although an optical monitoring campaign showed clear signs of gas variability, as noted by researchers earlier. However, the magnitude of circumstellar absorption in these systems is lower than observed toward β Pic.

Long Ca II monitoring campaigns of β Pic (e.g., Petterson & Tobin 1999), find significant short-term absorption variability. This variability can be explained by gas clouds very close to the star, which are caused by evaporating, star-grazing, km-sized objects, simply referred to as, Falling Evaporating Bodies (FEB’s; Beust 1994). A strong “stable” component, at rest in the stellar reference frame, is also detected toward β Pic (e.g., Crawford et al. 1994). The distribution of gas in this component, contrary to the variable component located very close to the star, is dispersed throughout the extended dust disk (Brandeker et al. 2004).

A “stable” absorption component in a gas phase resonance line can be caused by either intervening circumstellar or interstellar gas. Measuring the interstellar medium (ISM) along the line of sight and in the locality surrounding a circumstellar disk candidate, is critical to characterizing any “contaminating” ISM absorption (Crawford 2001; Redfield et al. 2007). In particular, the Sun resides in a large scale ISM structure known as the Local Bubble, whose boundary at ~ 100 pc is defined by a significant quantity of interstellar material (Lallement et al. 2003). If a “stable” absorption component is observed at the stellar radial

velocity, and similar absorption is not detected toward any proximate stars, it is likely that the absorption component is caused by circumstellar material.

Using near-infrared scattered light observations taken with the *Hubble Space Telescope*, Schneider, Silverstone, & Hines (2005) discovered that the debris disk surrounding HD32297 has an edge-on orientation. Disk emission extends out to ~ 400 AU in their observations, while radii < 33.6 AU are occulted by the coronagraphic obstacle. Optical scattered light observations by Kalas (2005) confirmed this orientation and extended the range of disk emission to ~ 1680 AU. The edge-on orientation of HD32297 makes it an ideal target for gas phase absorption measurements.

2. Observations

Observations of the Na I D doublet (5895.9242 and 5889.9510 Å) toward HD32297 were made over several epochs. The Na I doublet is among the strongest transitions in the optical wavelength band, appropriate for observing interstellar (Redfield 2006) and circumstellar (Lagrange-Henri et al. 1990b) absorption toward nearby stars. In addition, several stars in close angular proximity to HD32297 were observed, in order to reconstruct the ISM absorption profile along the line of sight. Stellar parameters of the observed targets are given in Table 1, and the observational parameters are listed in Table 2.

High resolution optical spectra were obtained using the Coudé Spectrometer on the 2.7m Harlan J. Smith Telescope at McDonald Observatory. The spectra were obtained at a resolution of $R \equiv \lambda/\Delta\lambda \sim 240,000$, using the 2dcoudé Spectrograph (Tull et al. 1995) in the CS21 configuration. The data were reduced using Image Reduction and Analysis Facility (IRAF; Tody 1993) and Interactive Data Language (IDL) routines to subtract the bias, flat field the images, remove scattered light and cosmic ray contamination, extract the echelle orders, calibrate the wavelength solution, and convert to heliocentric velocities. Wavelength calibration images were taken using a Th-Ar hollow cathode before and after each target.

Numerous weak water vapor lines are commonly present in spectra around the Na I doublet, and must be modeled and removed, in order to measure an accurate interstellar (or circumstellar) Na I absorption profile. I use a forward modeling technique demonstrated by Lallement et al. (1993) to remove telluric line contamination in the vicinity of the Na I D lines, with a terrestrial atmosphere model (AT - Atmospheric Transmission program, from Airhead Software, Boulder, CO) developed by Erich Grossman. With two Na I absorption lines, it is straightforward to identify contaminating telluric absorption.

All absorption lines were fit using standard methods (e.g., §2.2 in Redfield & Linsky

2004). Gaussian absorption components are fit to both Na I D lines simultaneously using atomic data from Morton (2003), and then convolved with the instrumental line spread function. Fitting the lines simultaneously reduces the influence of systematic errors, such as continuum placement and contamination by weak telluric features. The free parameters are the central velocity (v), the line width or Doppler parameter (b), and the column density (N) of Na I ions along the line of sight. The fits are shown in Figure 1 and fit parameters with 1σ statistical errors are listed in Table 2.

In addition, the spectra were used to estimate the stellar radial velocity (v_R) and projected stellar rotation ($v \sin i$) for HD32297, BD+07 777s, and BD+07 778 (see Table 1), quantities not listed in SIMBAD for these targets. The radial velocities of all 3 objects differ significantly, and therefore it is unlikely that they are physically associated. Note that the radial velocity of HD32297 ($v_R \sim +20 \text{ km s}^{-1}$) is measured from broad Na I and H α stellar absorption lines, and therefore is not tightly constrained.

3. Identification of Circumstellar Absorption Toward HD32297

The left column of Figure 1 shows that Na I absorption is clearly detected toward HD32297 in 5 observations over 5 months. Two components are easily distinguished, a strong component at $\sim 24.5 \text{ km s}^{-1}$ and a weaker component at $\sim 20.5 \text{ km s}^{-1}$. The Na I spectral region for 5 stars in close angular proximity to HD32297 is also shown in Figure 1. Only a single ISM component, at $\sim 24.2 \text{ km s}^{-1}$, is detected in the 3 distant neighbors, indicating that large scale interstellar material is located at a distance between 59.4–112 pc. All targets located beyond this material, including HD32297, should have a similar ISM absorption feature. This strong ISM absorption is probably associated with the boundary material of the Local Bubble, which is estimated to be $\sim 90 \text{ pc}$ in this direction (Lallement et al. 2003). If located at this distance, the physical separation of the interstellar material observed toward HD32297 and the material toward BD+07 777s ($\Delta\theta = 0'.9$) is 0.025 pc, BD+07 778 ($2'.4$) is 0.064 pc, and 18 Ori ($5'.1$) is 8.1 pc. Toward HD32297’s two closest neighbors, the ISM absorption is almost identical in projected velocity and column density to the strong absorption seen toward HD32297, while toward 18 Ori, the absorption differs slightly in both v and N , indicating that any small scale morphological variations in the Local Bubble shell are on scales $>0.1 \text{ pc}$ but $<8 \text{ pc}$. Small scale variations in the Local Bubble shell have been detected by Redfield, Scalo, & Smith (2006) on scales $\sim 0.5 \text{ pc}$.

It is unlikely that the unique 20.5 km s^{-1} feature observed toward HD32297 is caused by a small scale interstellar structure. Although small ISM structures (0.01–2.0 pc) have been observed (e.g., Ferlet, Dennefeld, & Maurice 1985; Meyer & Blades 1996), it is more likely

that the unique feature is due to absorption in the circumstellar environment surrounding HD32297 because (1) HD32297 is known to be an edge-on debris disk, (2) no similar absorption is detected in the very close neighboring sightlines (0.03–0.08 pc), and (3) the absorption matches the stellar radial velocity.

4. Temporal Variability of Circumstellar Component

Temporal variability is also a hallmark of circumstellar material (e.g., Ferlet, Vidal-Madjar, & Hobbs 1987, Petterson & Tobin 1999, Redfield et al. 2007). To search for variability, Figure 2 shows difference spectra of all observations. Some indication of temporal variability on time scales of months is detected. For example, between the 2005 Sep and 2006 Feb observations, the $\sim 20.5 \text{ km s}^{-1}$ feature became stronger and the separation between the circumstellar and interstellar features became less distinct, despite the fact that the 2006 Feb observations were made at a slightly higher resolving power. The redshifted variability seen between 2005 Sep and 2006 Feb is $\sim 5\sigma$ above the standard deviation. The same pattern is seen in both Na I lines, indicating that the telluric contamination is not causing the variation. Slight changes in the resolving power of our instrument could mimic this variable behavior, differentially moving light from the cores of the line to the wings (or vice versa). However, resolution variability should cause (1) symmetric features in the wings of the line whereas we see a feature only to the blue of the ISM feature and not to the red, and (2) should have a stronger effect on stronger absorption features, whereas the feature is roughly identical in both lines, which could be caused if the absorbing material covers only a fraction of the stellar disk, as has been seen toward β Pic (Vidal-Madjar et al. 1994).

This data alone provides only a subtle indication of temporal variation in Na I, partially because any significant absorption toward the red, is masked by the strong ISM feature. Redshifted circumstellar absorption dominates the Ca II gas absorption variability toward β Pic (e.g., Petterson & Tobin 1999), while no temporal variability has ever been detected in Na I toward β Pic, only the “stable” absorption component is seen in this ion (Welsh et al. 1997). Circumstellar variability in Na I has been detected in other edge-on debris disks, e.g., β Car, HD85905, and HR10 (Welsh et al. 1998; Redfield et al. 2007). Any redshifted absorption occurring in this object could cause fluctuations in the measured column density of the “constant” ISM feature. Little evidence for variability is found toward the blue.

5. Gas Disk Mass

These observations indicate that HD32297 has the strongest Na I circumstellar disk signature detected around a nearby main sequence debris disk star. Even compared to β Pic, the prototypical edge-on debris disk with Na I absorption column densities of $\log N_{\text{NaI}} \sim 10.69$ – 10.73 (Hobbs et al. 1985; Welsh et al. 1997), the gas disk around HD32297, with $\log N_{\text{NaI}} \sim 11.4$, has $5\times$ the Na I column density. A crude estimate of the gas mass surrounding HD32297 can be made if it is assumed to have the same morphology and abundances as the stable gas around β Pic. Although the observations of HD32297 indicate some red-shifted temporal variability, much of the gas is stable over all observations. Using β Pic as a proxy, the variable gas is likely located very close to the star (Lagrange, Backman, & Artymowicz 2000), while the stable gas at rest in the stellar frame, likely traces the bulk dust disk (Brandeker et al. 2004). For this calculation, I assume all the gas is in the stable component, and therefore this gas mass estimate should be considered an upper limit. The morphology of the disk is assumed to follow a broken power law density profile, as fit to the Na I emission profile of the β Pic disk (see Equation 1 of Brandeker et al. 2004), and assumed to extend out to the edge of the debris disk at ~ 1680 AU (Kalas 2005). The abundances in the HD32297 disk are assumed to be similar to β Pic (Roberge et al. 2006), where the ratio $N(\text{H I})/N(\text{Na I}) \lesssim 8.8 \times 10^8$, is based on β Pic Na I measurements by Brandeker et al. (2004) and H I limits by Freudling et al. (1995). Given these assumption, I calculate a gas mass, distributed through the bulk debris disk surrounding HD32297 at $M_{\text{gas}} \sim 0.3M_{\oplus}$.

Future observations are planned to continue monitoring the temporal variability of the circumstellar gas toward HD32297 to determine the ratio of stable to variable gas, and measure the Ca II gas disk absorption, in order to independently measure the Ca II to Na I ratio. A more definitive detection of temporal variability may require monitoring excited lines which will show circumstellar absorption, but not the strong interstellar feature.

6. Conclusions

I present the first high resolution optical spectra of the Na I doublet toward the debris disk HD32297 and stars in close angular proximity. A summary of results include:

(1) Two absorption components are detected toward HD32297, while only one is detected toward its proximate neighbors located at a comparable distance. The extra absorption component in the spectrum of HD32297, which is also at rest in the stellar reference frame, is therefore likely caused by circumstellar material.

(2) The ISM absorption is similar among HD32297 and its two closest neighbors, and is

likely due to absorption from the shell that defines the boundary of the Local Bubble. Some variation in Local Bubble absorption is detected toward 18 Ori.

(3) Radial velocities of HD32297, BD+07 777s, and BD+07 778 are measured and differ significantly, indicating that they are likely not physically associated.

(4) Some indication of temporal variability is detected over several epochs of observations. Instrumental resolution variations and masking by the strong ISM absorption, make a definitive detection of circumstellar Na I variability difficult.

(5) The measured circumstellar feature toward HD32297 ($\log N_{\text{NaI}} \sim 11.4$) is the strongest such absorption measured toward any nearby main sequence debris disk, ~ 5 times greater than the column density of the prototypical edge-on debris disk, β Pic.

(6) If the morphology and abundances of the stable gas component around HD32297 are assumed to be similar to β Pic, I estimate an upper limit to the gas mass in the circumstellar disk surrounding HD32297 of $\sim 0.3 M_{\oplus}$.

Support for this work was provided by NASA through Hubble Fellowship grant HST-HF-01190.01 awarded by the Space Telescope Science Institute, which is operated by the Association of Universities for Research in Astronomy, Inc., for NASA, under contract NAS 5-26555. I would like to thank D. Doss, G. Harper, and A. Brown, for their assistance with these observations. The insightful comments by the anonymous referee were very helpful.

Facilities: Smith (CS21)

REFERENCES

- Aumann, H. H., et al. 1984, ApJ, 278, L23
- Backman, D. E., & Paresce, F. 1993, in Protostars and Planets III, ed. E. H. Levy & J. I. Lunine, 1253–1304
- Beust, H. 1994, in Circumstellar Dust Disks and Planet Formation, ed. R. Ferlet & A. Vidal-Madjar (Gif sur Yvette Cedex: Editions Frontières), 35
- Brandeker, A., Liseau, R., Olofsson, G., & Fridlund, M. 2004, A&A, 413, 681
- Crawford, I. A. 2001, MNRAS, 327, 841
- Crawford, I. A., Spyromilio, J., Barlow, M. J., Diego, F., & Lagrange, A. M. 1994, MNRAS, 266, L65
- Ferlet, R., Dennefeld, M., & Maurice, E. 1985, A&A, 152, 151

- Ferlet, R., Vidal-Madjar, A., & Hobbs, L. M. 1987, *A&A*, 185, 267
- Freudling, W., Lagrange, A.-M., Vidal-Madjar, A., Ferlet, R., & Forveille, T. 1995, *A&A*, 301, 231
- Hobbs, L. M., Vidal-Madjar, A., Ferlet, R., Albert, C. E., & Gry, C. 1985, *ApJ*, 293, L29
- Kalas, P. 2005, *ApJ*, 635, L169
- Kalas, P., Liu, M. C., & Matthews, B. C. 2004, *Science*, 303, 1990
- Lagrange, A.-M., Backman, D. E., & Artymowicz, P. 2000, in *Protostars and Planets IV*, ed. V. Mannings, A. P. Boss, & S. S. Russell (Tucson: Univ. Arizona Press), 639
- Lagrange-Henri, A. M., Beust, H., Ferlet, R., Vidal-Madjar, A., & Hobbs, L. M. 1990a, *A&A*, 227, L13
- Lagrange-Henri, A. M., Ferlet, R., Vidal-Madjar, A., Beust, H., Gry, C., & Lallement, R. 1990b, *A&AS*, 85, 1089
- Lallement, R., Bertin, P., Chassefiere, E., & Scott, N. 1993, *A&A*, 271, 734
- Lallement, R., Welsh, B. Y., Vergely, J. L., Crifo, F., & Sfeir, D. 2003, *A&A*, 411, 447
- Meyer, D. M., & Blades, J. C. 1996, *ApJ*, 464, L179
- Morton, D. C. 2003, *ApJS*, 149, 205
- Petterson, O. K. L., & Tobin, W. 1999, *MNRAS*, 304, 733
- Redfield, S. 2006, in *ASP Conf. Ser. 352, New Horizons in Astronomy*, Frank N. Bash Symposium 2005, ed. S. J. Kannappan, S. Redfield, J. E. Kessler-Silacci, M. Landriau, & N. Drory (San Francisco: ASP), 79
- Redfield, S., Kessler-Silacci, J. E., & Cieza, L. A. 2007, *ApJ*, submitted
- Redfield, S., & Linsky, J. L. 2004, *ApJ*, 602, 776
- Redfield, S., Scalo, J., & Smith, D. S. 2006, in *ASP Conf. Ser., Small Ionized and Neutral Structures in the Diffuse ISM*, ed. W. M. Goss (San Francisco: ASP), in press
- Roberge, A., Feldman, P. D., Weinberger, A. J., Deleuil, M., & Bouret, J.-C. 2006, *Nature*, 441, 724
- Roberge, A., Weinberger, A. J., Redfield, S., & Feldman, P. D. 2005, *ApJ*, 626, L105

Schneider, G., Silverstone, M. D., & Hines, D. C. 2005, *ApJ*, 629, L117

Smith, B. A., & Terrile, R. J. 1984, *Science*, 226, 1421

Tody, D. 1993, in *ASP Conf. Ser. 52: Astronomical Data Analysis Software and Systems II*, ed. R. J. Hanisch, R. J. V. Brissenden, & J. Barnes (San Francisco: ASP), 173

Tull, R. G., MacQueen, P. J., Sneden, C., & Lambert, D. L. 1995, *PASP*, 107, 251

Vidal-Madjar, A., et al. 1994, *A&A*, 290, 245

Welsh, B. Y., Craig, N., Crawford, I. A., & Price, R. J. 1998, *A&A*, 338, 674

Welsh, B. Y., Craig, N., Jelinsky, S., & Sasseen, T. 1997, *A&A*, 321, 888

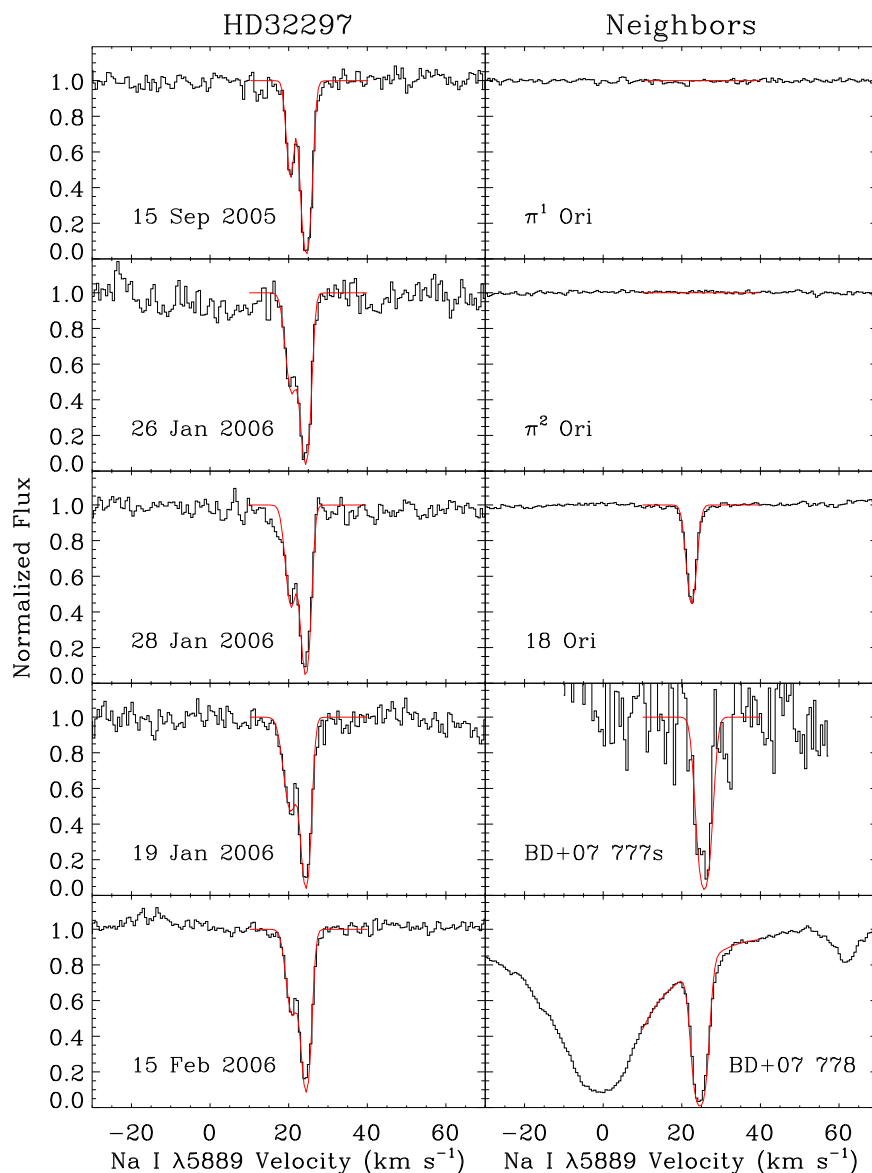


Fig. 1.— Na I absorption lines toward HD32297 (*left*) and toward stars proximate to HD32297 (*right*). All spectra are flux normalized such that stellar features are removed, except for BD+07 778, where the stellar feature is retained. All objects beyond 60 pc, including HD32297, show a significant interstellar component at ~ 24.5 km s $^{-1}$, whereas only HD32297 has an additional absorption feature ~ 20.5 km s $^{-1}$, presumably circumstellar. Temporal variability can be seen in the circumstellar component and redward in HD32297 over several observational epochs. The absorption in both lines of the Na I doublet is fit simultaneously. The best fit, convolved with the line spread function, is overplotted (red).

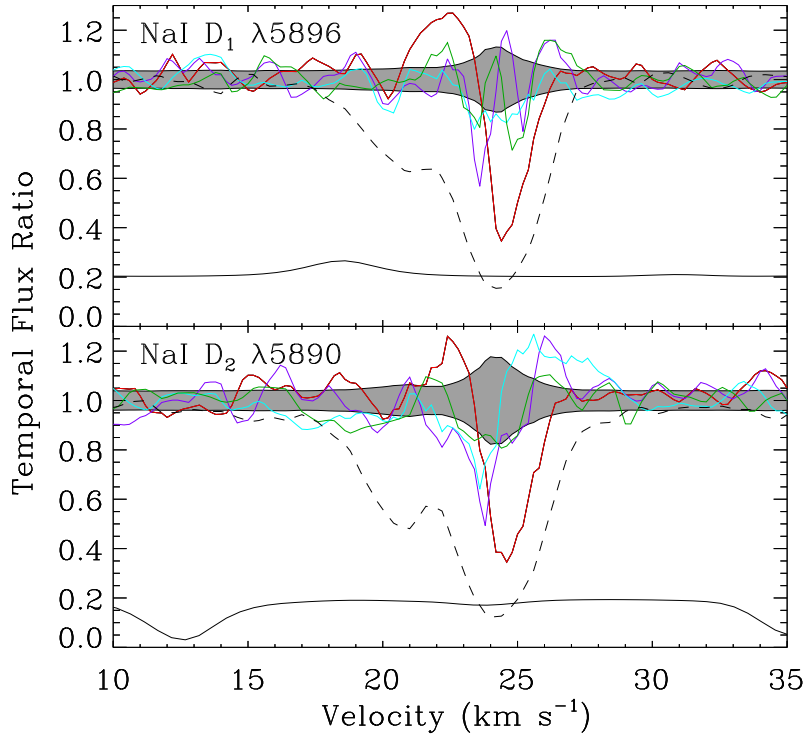


Fig. 2.— Difference spectra of all HD32297 observations for both Na I lines, relative to the final spectrum taken 2006 Feb 15, which is plotted as the dashed line. The gray shaded region indicates the ratio error band. The ratio of the telluric water vapor spectra of 2005 Sep 15 and 2006 Feb 15 is shown offset toward the bottom of each plot. The most notable temporal variation occurs between the 2005 Sep 15 observation (red), where the flux variation, centered at $\sim 22.5 \text{ km s}^{-1}$, is $\sim 5\sigma$. This redshifted variability is common in gas absorption toward edge-on debris disks, although in this particular instance the variability is partially masked by the strong ISM component.

Table 1. Stellar Parameters for HD32297 and Nearby Stars^a

HD #	Other Name	Spectral Type	m_V (mag)	v_R (km s ⁻¹)	$v \sin i$ (km s ⁻¹)	l (deg)	b (deg)	Distance ^b (pc)	$\Delta\theta$ (deg)	Δr_{pos}^c (pc)
32297	BD+07 777	A0	8.13	$\sim +20^d$	$\sim 80^d$	192.83	-20.17	112^{+15}_{-12}	0.0000	0.0
...	BD+07 777s	G0 ^e	10.2	-55 ^d	$\sim 2^d$	192.85	-20.17	...	0.0156	0.030
32304	BD+07 778	G5	6.87	-1.4 ^d	$\sim 3.5^d$	192.88	-20.17	134^{+19}_{-15}	0.0406	0.079
30739	π^2 Ori	A1Vn	4.35	+24	212	189.82	-21.83	$59.4^{+4.9}_{-4.2}$	3.2653	3.4
31295	π^1 Ori	A0V	4.66	+13	120	189.35	-20.25	$37.0^{+1.3}_{-1.2}$	3.2748	2.1
34203	18 Ori	A0V	5.52	-8.2	70	191.29	-15.25	$112.9^{+10.4}_{-8.8}$	5.1306	10.1

^aAll values from SIMBAD unless otherwise noted.

^bDistances calculated from *Hipparcos* parallaxes.

^cPhysical separation in the plane of the sky from HD32297, at the distance of the closest partner.

^dMeasured from spectra presented in this paper.

^eSpectral type based on $B - V = 0.57$.

Table 2. Observational and Absorption Fit Parameters for HD32297 and Nearby Stars

HD #	Other Name	Date	$v_{\text{atm}}^{\text{a}}$ (km s ⁻¹)	$\langle FWHM_{\text{ThAr}} \rangle^{\text{b}}$ (km s ⁻¹)	S/N ^c	v (km s ⁻¹)	b (km s ⁻¹)	log N (cm ⁻²)
32297	BD+07 777	2005 Sep 15	+28.2	1.565	31	20.459 ± 0.030	0.38 ± 0.28	10.97 ^{+0.25} _{-0.67}
						24.546 ± 0.012	0.742 ± 0.063	12.388 ^{+0.083} _{-0.103}
32297	BD+07 777	2006 Jan 26	-22.8	1.253	17	20.50 ± 0.27	1.23 ± 0.55	11.384 ± 0.077
						24.30 ± 0.12	0.84 ± 0.21	12.16 ^{+0.12} _{-0.16}
32297	BD+07 777	2006 Jan 28	-23.4	1.266	22	20.48 ± 0.23	1.24 ± 0.42	11.449 ^{+0.053} _{-0.060}
						24.34 ± 0.17	0.82 ± 0.31	11.98 ^{+0.25} _{-0.64}
32297	BD+07 777	2006 Jan 29	-23.7	1.288	20	20.42 ± 0.20	1.71 ± 0.28	11.454 ^{+0.049} _{-0.050}
						24.424 ± 0.086	0.71 ± 0.23	12.02 ^{+0.18} _{-0.32}
32297	BD+07 777	2006 Feb 15	-27.5	1.199	39	20.51 ± 0.26	1.14 ± 0.41	11.297 ^{+0.097} _{-0.120}
						24.41 ± 0.13	0.94 ± 0.30	11.97 ^{+0.15} _{-0.20}
...	BD+07 777s	2006 Feb 16	-27.7	1.238	6	25.55 ± 0.28	1.581 ± 0.078	12.03 ^{+0.12} _{-0.18}
32304	BD+07 778	2006 Feb 16	-27.7	1.244	52	24.583 ± 0.083	1.65 ± 0.15	12.18 ^{+0.12} _{-0.16}
30739	π ² Ori	2006 Feb 16	-28.3	1.213	133	< 9.8
31295	π ¹ Ori	2004 Oct 18	+21.1	1.761	100	< 10.1
34203	18 Ori	2006 Feb 15	-27.3	1.189	117	22.464 ± 0.022	1.150 ± 0.036	11.403 ^{+0.040} _{-0.044}

^aProjected velocity of the Earth’s atmosphere.

^bResolution based on neighboring ThAr comparison lamp spectra assuming that the ThAr lines are fully resolved.

^cSignal-to-noise at core of NaI absorption line.